Computers & Geosciences 155 (2021) 104864

Contents lists available at ScienceDirect

Computers and Geosciences

journal homepage: www.elsevier.com/locate/cageo

Research paper

GROOPS: A software toolkit for gravity field recovery and GNSS processing

Torsten Mayer-Gürr [a], Saniya Behzadpour [a], Annette Eicker [b], Matthias Ellmer [a,c], Beate Koch [a], Sandro Krauss [a], Christian Pock [a,d], Daniel Rieser [a], Sebastian Strasser [a], Barbara Süsser-Rechberger [a], Norbert Zehentner [a], Andreas Kvas [a,*]

[a] Graz University of Technology, Institute of Geodesy, Steyrergasse 30, 8010 Graz, Austria
[b] HafenCity University Hamburg, Überseeallee 16, 20457 Hamburg, Germany
[c] Jet Propulsion Laboratory, California Institute of Technology, Pasadena, CA, USA
[d] KNAPP AG - Logistics, Günter Knapp-Straße 5-7, 8075 Hart bei Graz, Austria

ARTICLE INFO

Keywords:
Gravity field recovery
GNSS processing
Orbit determination

ABSTRACT

The Gravity Recovery Object Oriented Programming System (GROOPS) is a software toolkit written in C++ that enables the user to perform core geodetic tasks. Key features of the software include gravity field recovery from satellite and terrestrial data, the determination of satellite orbits from global navigation satellite system (GNSS) measurements, and the computation of GNSS constellations and ground station networks. Next to raw data processing, GROOPS is capable to operate on time series and spatial data to directly analyze and visualize the computed data sets. Most tasks and algorithms are (optionally) parallelized through the Message Passing Interface, thus the software enables a smooth transition from single-CPU desktop computers to large distributed computing environments for resource intensive tasks. For an easy and intuitive setup of complex workflows, GROOPS contains a graphical user interface to create and edit configuration files. The source code of the software is freely available on GitHub (https://github.com/groops-devs/groops) together with documentation, a cookbook with guided examples, and step-by-step installation instructions.

1. Introduction

The determination of Earth's geometric shape, orientation in space, and gravity field are core geodetic tasks and provide the basis for a wide range of Earth sciences. A stable geometric reference frame allows long-term observations of critical processes such as sea level rise, tectonic plate motion, and post-glacial rebound (Le Cozannet et al., 2015; Nerem et al., 2000; Blewitt et al., 2010). Earth's static gravity field is a key quantity for oceanographic and geological sciences (Bingham et al., 2014; Johannessen et al., 2003; Ebbing et al., 2018). Temporal changes in gravitational attraction can be used to infer mass changes on Earth's surface caused by, for example, the continental water cycle, ocean currents, or melting ice caps and glaciers (Chambers, 2006; Velicogna, 2009; Chen et al., 2010; Tapley et al., 2019) and provide key insights into these climate-relevant processes.

The derivation of these quantities is typically very resource intensive, that is, a vast number of measurements from different observation techniques need to be combined and processed. As a consequence, dedicated software packages, both for research and commercial purposes, have been developed (e.g., Dach et al., 2015; Böhm et al., 2018; Bertiger et al., 2020).

In this article we present the Gravity Recovery Object Oriented Programming System (GROOPS), a software toolkit for performing core geodetic tasks. The source code of GROOPS is publicly available on GitHub (https://github.com/groops-devs/groops) together with a comprehensive documentation and an installation guide. GROOPS is written in C++ and is designed to be operating system independent. It can be compiled and run on both Linux, Microsoft Windows, and macOS. To enable an intuitive interaction with the software, GROOPS includes a graphical user interface (GUI) also written in C++.

The feature set of GROOPS can be categorized into four parts:

- gravity field recovery from satellite and terrestrial observations
- processing of GNSS constellations and ground station networks to determine GNSS products
- orbit determination of low-Earth-orbiting (LEO) satellites
- statistical analysis of time series and spatial data sets

The methods implemented in the software are documented to a high degree in peer-reviewed articles (e.g., Pock et al., 2014; Zehentner and Mayer-Gürr, 2016; Kvas and Mayer-Gürr, 2019; Strasser et al., 2019; Ellmer and Mayer-Gürr, 2017) and theses (Ellmer, 2018; Kvas,

* Corresponding author.
E-mail address: kvas@tugraz.at (A. Kvas).

https://doi.org/10.1016/j.cageo.2021.104864
Received 23 December 2020; Received in revised form 7 June 2021; Accepted 7 June 2021
Available online 12 June 2021

2020). Data sets, which are the main output of GROOPS, have been used within the scientific community (e.g., Gouweleeuw et al., 2018; Humphrey and Gudmundsson, 2019; Eicker et al., 2020; Göttl et al., 2019; Jäggi et al., 2020). This means that they have undergone not only an internal pre-publication evaluation but also independent external evaluations.

2. Methods and results

2.1. Least squares adjustment

A common component in all features of GROOPS is the solution of overdetermined systems of equations in a least squares adjustment (LSA) with observation equations in the form

$$\mathbf{l} = \mathbf{A}\mathbf{x} + \mathbf{e}, \qquad \mathbf{e} \sim \mathcal{N}(\mathbf{0}, \boldsymbol{\Sigma}). \tag{1}$$

In Eq. (1), $\mathbf{l}$ is the vector of observations, $\mathbf{A}$ is the design matrix, $\mathbf{x}$ are the unknown parameters, $\mathbf{e}$ are the residuals, and $\boldsymbol{\Sigma}$ is the covariance matrix of the residuals. The LSA yields the solution $\hat{\mathbf{x}}$ which minimizes the objective function

$$\mathbf{e}^T \boldsymbol{\Sigma}^{-1} \mathbf{e} \rightarrow \min. \tag{2}$$

Typically, multiple observation groups are used to determine the unknown parameters, which can be written as

$$\begin{bmatrix} \mathbf{l}_1 \\ \vdots \\ \mathbf{l}_n \end{bmatrix} = \begin{bmatrix} \mathbf{A}_1 \\ \vdots \\ \mathbf{A}_n \end{bmatrix} \mathbf{x} + \begin{bmatrix} \mathbf{e}_1 \\ \vdots \\ \mathbf{e}_n \end{bmatrix}, \tag{3}$$

where $\mathbf{l}_i, \mathbf{A}_i$ are the observation equations of a single observation group. For example, these could be segments of a time series of observations, dubbed "arcs" in GROOPS, or a set of observations between a single GNSS satellite and receiver at one epoch.

Grouping observations has advantages both from an implementation and processing point of view. Predetermined observation groups are a natural entry point for parallelization, that is, processing steps during the setup of observation equation are likely to require no communication between processes. Furthermore, having individual observation groups allows to perform variance component estimation (VCE, Koch and Kusche, 2002) to properly determine the relative weights between possibly heterogeneous measurements. This approach is used throughout GROOPS with application-specific adaptions when necessary.

In order to determine the unknown parameters from the LSA, most applications in GROOPS assemble the system of normal equations $\mathbf{N}\hat{\mathbf{x}} = \mathbf{n}$, as opposed to using iterative solvers (e.g. Baur, 2009). Since $\mathbf{N}$ is symmetric, only one triangle needs to be kept in memory. In GROOPS, the upper triangle is chosen. Depending on the application, the size and structure of the coefficient matrix $\mathbf{N}$ varies. GNSS processing as implemented in GROOPS leads to a large and highly sparse least squares problem. For a global ground station network of 800 stations, 5 million parameters are set up, including station coordinates, transmitter and receiver clocks, and code and phase biases (cf. Section 2.3). Since most of these parameters are specific to a single satellite, receiver, or observation type, a large portion of the normal equation coefficient matrix remains zero. This leads to an overall sparsity of 99.5%.

To accommodate this special structure, the normal equation matrix in GROOPS is implemented as an object-oriented representation of a sparse block matrix $\mathbf{N} = (\mathbf{N}_{ij})$ with dense blocks $\mathbf{N}_{ij}$. Since the individual blocks are dense, the overall memory demand depends on the chosen block size. However, blocks should not be chosen too small as the efficiency of matrix–matrix operations decreases below a certain size (e.g., Goto and van de Geijn, 2006). Therefore, a trade-off between memory requirements and block size has to be made. In some cases, such as the GNSS processing example mentioned above, this may lead to a large number of blocks and subsequently significant overhead in managing the block matrix $\mathbf{N}$.

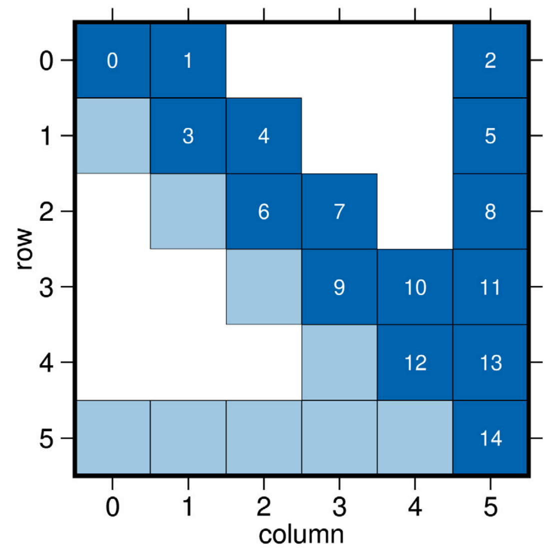

Fig. 1. Schematic representation of the sparse block matrix storage scheme implemented in GROOPS. The number in each block represents the index k in the block list. The lower triangle depicted in light blue is not kept in memory. (For interpretation of the references to color in this figure legend, the reader is referred to the web version of this article.)

Table 1
Contents of the data structure `index_per_row` which stores non-zero blocks per row.

row	(column, list index)		
0	(0, 0)	(1, 1)	(5, 2)
1	(1, 3)	(2, 4)	(5, 5)
2	(2, 6)	(3, 7)	(5, 8)
3	(3, 9)	(4, 10)	(5, 11)
4	(4, 12)	(5, 13)	
5	(5, 14)		

For large problems it is beneficial to set up the normal equations on a computer cluster using multiple parallel processes as the number of observations and parameters exceed the memory capacity of a standard desktop computer. The matrix blocks are per default distributed in block-cyclic fashion (e.g., Blackford et al., 1997) among the processes and stored as an unsorted list. Pairs ($\mathbf{N}_{ij}$, r) consisting of the matrix block and the rank of the assigned process r are appended to this list in the order the blocks $\mathbf{N}_{ij}$ are initialized.

To provide a convenient mapping from row i and column j to the list index k of the corresponding matrix block, two concurrent data structures are used. One stores the column and list index per row, that is `index_per_row[i]` returns a list of pairs (j, k) for all non-zero blocks in row i. The second one contains the row and list index per column, `index_per_column[j]` returns a list of pairs (i, k) for all non-zero blocks in column j.

To illustrate this storage scheme, Fig. 1 shows a schematic view of a distributed normal equation matrix with a typical block structure. In this example, the blocks are initialized row-wise starting in the upper left corner. The contents of the data structures that map row and column to the list index are shown in Tables 1 and 2. Since the block row is the primary index in the first data structure, we can directly access the list which contains the column and list index of all non-zero blocks for any given row. Similarly, as the block column is the primary index in the second data structure, we get a list of all non-zero blocks in the given column. In the current example this means that `index_per_row[1]` returns a list of three pairs: (1, 3), (2, 4), and (5, 5). Similarly, `index_per_column[4]` returns a list of two pairs: (3, 10) and (4, 12).

While this storage scheme is redundant, keeping both row and column indices has benefits in certain circumstances. In blocked linear

Table 2
Contents of the data structure `index_per_column` which stores non-zero blocks per column.

column	(row, list index)					
0	(0, 0)					
1	(0, 1)	(1, 3)				
2	(1, 4)	(2, 6)				
3	(2, 7)	(3, 9)				
4	(3, 10)	(4, 12)				
5	(0, 2)	(1, 5)	(2, 8)	(3, 11)	(4, 13)	(5, 14)

algebra algorithms, operations involving all non-zero blocks of a block row or block column are very common. Depending on whether a block row or a block column needs to be addressed, the container with the respective key can be directly accessed. This avoids iterating over all rows to find the non-zero blocks of a specific column or iterating over all columns to find the non-zero blocks of a specific row. Thus the overhead for operations involving the block matrix $\mathbf{N}$ is kept low even for cases where $\mathbf{N}$ is highly sparse and comprised of a large number of blocks.

Gravity field recovery, as opposed to GNSS processing, typically yields smaller and dense normal equation coefficient matrices where such optimizations are not strictly necessary. Still, all features in GROOPS make use of the same underlying sparse matrix structure, thus maximizing code reuse.

Solving the system of normal equations in GROOPS is implemented by performing an in-place Cholesky decomposition of $\mathbf{N}$ followed by forward and back substitution. These operations are implemented as parallel block algorithms following Choi et al. (1996). We briefly note here that the Cholesky decomposition of $\mathbf{N}$ potentially changes the sparsity structure of the distributed matrix. Depending on the application this can increase the memory demands by orders of magnitude, thus making the solution to the least squares problem not feasible. In GROOPS parameters are ordered to yield a kite structure (Schuh, 1996; Boxhammer and Schuh, 2006; Tewarson and Cheng, 1973), which minimizes the number of fill-in elements and largely retains the initial non-zero block structure.

Next to the algorithms to solve the symmetric system of equations, GROOPS supports the computation of the full variance–covariance matrix of the estimated parameters, that is, the inverse of the normal equation coefficients matrix. For large, sparse systems it cannot be guaranteed that the inverse normal equation matrix will fit into memory, as in the inversion process zero blocks will be filled (Boxhammer and Schuh, 2006). To avoid this behavior, GROOPS also supports a parallel sparse inversion algorithm, which retains the sparsity structure of the Cholesky factor based on an algorithm for block-banded matrices introduced by Asif and Moura (2005).

2.2. Global gravity field recovery from satellite data

Gravity field recovery from satellite data within GROOPS is based on the short-arc approach introduced by Mayer-Gürr (2006) and solves Newton's equation of motion through variational equations (Montenbruck and Gill, 2000). A detailed overview of the algorithms used on the example of the Gravity Recovery and Climate Experiment (GRACE) satellite mission can be found in Ellmer (2018, section 5).

A typical workflow starts with converting data files as well as metadata and auxiliary data into internal file formats. This has the advantage that multiple satellite missions, where data file formats in general vary drastically, can be ingested in the same fashion by the same programs. Then, the input data is quality controlled and checked for outliers. This can be done with criteria based on metadata, thresholds or robust sample statistics.

In the next step, the least squares adjustment, which we use to solve for the unknown gravity field, is set up. Here, we can also determine the noise characteristics of the input data using variance

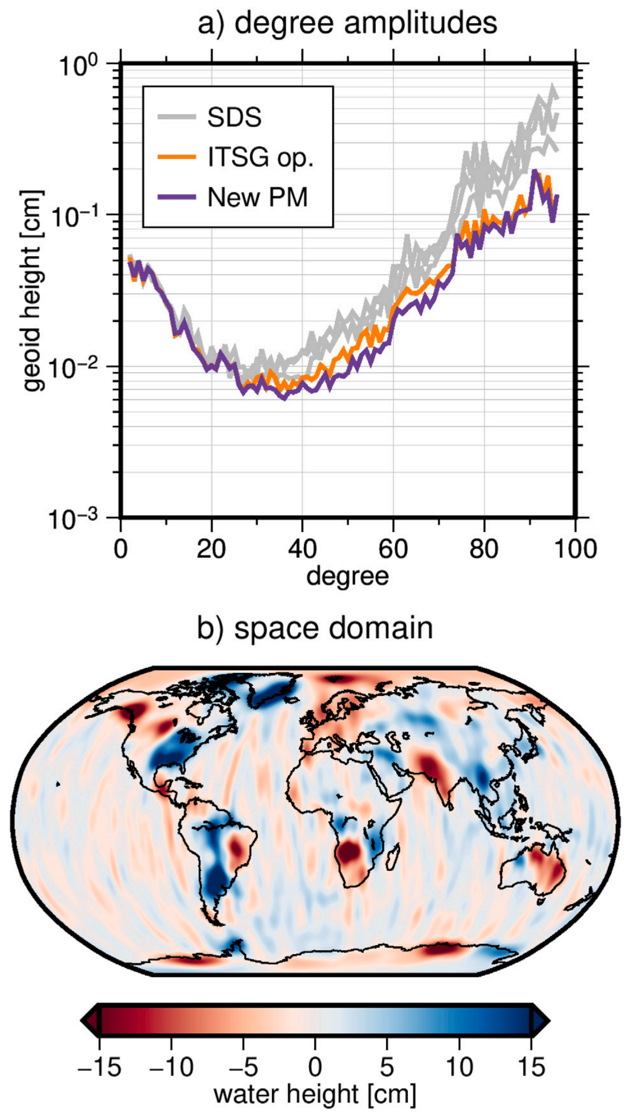

Fig. 2. (a) Comparison of GRACE Follow-On solutions from the official science data systems (SDS) and solutions computed with GROOPS (ITSG op., New PM) in spectral domain. (b) Estimated gravity field solution in space domain expressed as equivalent water height.

component estimation. The result of this processing step is either the least squares solution of the gravity field or additionally the system of normal equations, which can be stored as a file for further processing.

Finally, post-processing steps such as restoring background models can be performed and the solution is converted from the internal file format to a standardized file format for publication and exchange. Optionally, the result can be visualized and evaluated through, for example, intercomparison with other solutions. Fig. 2a shows an example of such an intercomparison of GRACE Follow-On (GRACE-FO) solutions in terms of degree amplitudes. Two solutions computed with GROOPS (ITSG op., New PM) are compared with the ensemble of GRACE-FO Science Data System (SDS) solutions. Alternatively, the obtained solution can also be visualized in space domain (see Fig. 2b). Depending on the resolution of gravity field solution, the transformation between spectral and spatial domain is very resource intensive (Hirt et al., 2014) and thus is parallelized.

GROOPS is capable of dealing with different observation types such as orbit positions derived from raw GNSS measurements, highly accurate intersatellite ranging observations as realized within the GRACE

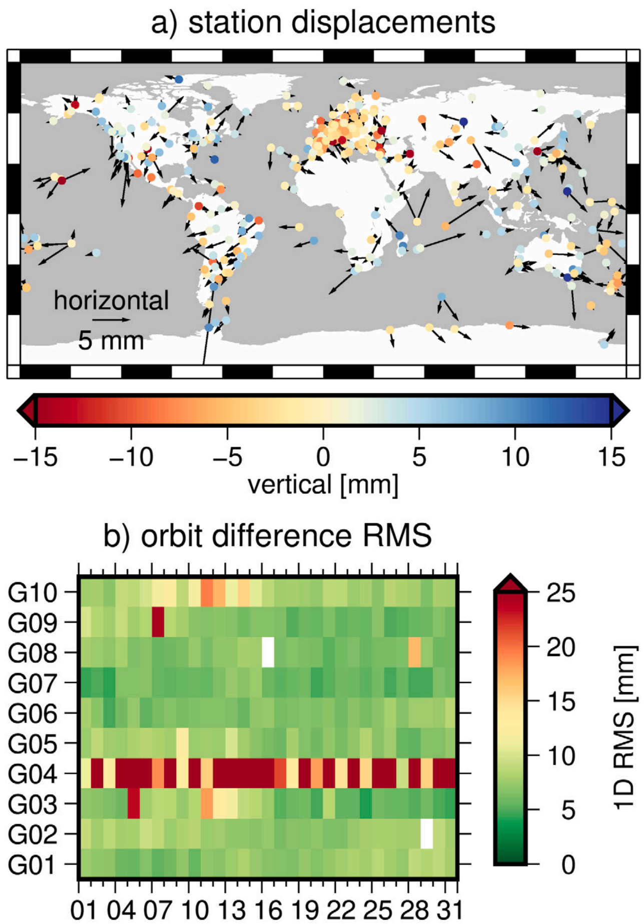

Fig. 3. (a) Differences of station coordinates derived by GROOPS to IGS combination for 2019-08-01 in terms of horizontal and vertical displacements. (b) Root mean square (RMS) of daily GPS satellite orbit differences between GROOPS-derived and IGS combined solutions for August 2019.

mission and its successor GRACE-FO, and gradiometer observations of the Gravity field and steady-state Ocean Circulation Explorer (GOCE).

Published global gravity field solutions computed with GROOPS include the ITSG-Grace time series (Kvas et al., 2019a); GOCO06s (Kvas et al., 2019b, 2020), a static gravity field model based on 1.2 billion observations from 19 satellites; and a lunar gravity field model (Wirnsberger et al., 2019). These data sets have been widely used within the geodetic and geophysical community and have undergone extensive internal and external evaluation (Bonin and Save, 2020; Göttl et al., 2019; Meyer et al., 2019; Ghobadi-Far et al., 2020). From this we can conclude that GROOPS is capable of producing state-of-the-art gravity field data products.

Next to global gravity field recovery, the determination of regional gravity field solutions from terrestrial data is also possible and has been successfully performed for the geoid of Austria (Pock et al., 2014). The approach implemented in GROOPS makes use of radial basis functions (Eicker et al., 2013), where the regional gravity field is parametrized as quasi-localized splines.

2.3. GNSS processing

GROOPS uses the raw observation approach (Schönemann et al., 2011; Schönemann, 2014) as detailed in Strasser et al. (2019) to process observations from a global GNSS station network to multiple satellite constellations. These include the U.S. Global Positioning System (GPS), the Russian Global Navigation Satellite System (GLONASS), the European system Galileo, and the Chinese BeiDou Navigation Satellite System (BDS) as well as the Japanese Quasi-Zenith Satellite System (QZSS).

Many geodetic, geophysical, and environmental applications require high-precision GNSS products such as satellite orbits, satellite clocks, or station positions. They are the prerequisite for high-quality satellite orbits of many remote sensing satellites, form the basis for local and regional surveys (Harpham et al., 2016), and enable new measurement techniques (Cooper et al., 2019). Different analysis centers routinely generate such data sets under the umbrella of the International GNSS Service (IGS, Johnston et al., 2017).

GNSS processing relies on a large and diverse set of data and metadata. GROOPS offers programs to convert such data and metadata from file formats widely used in the GNSS community, for example RINEX, SINEX, and ANTEX, to internal file formats optimized for usability in the core GNSS programs. Data and metadata is mostly stored in individual files per satellite/station. This reduces the amount of specialization required in the code base, as satellites/stations only differ by parameters and values sourced from their respective files. Furthermore, it increases the compatibility with general GROOPS programs that are designed to work with data from individual instruments.

Once all data and metadata are prepared, the first step in GNSS orbit determination and network processing is the numerical integration of the satellite orbits. Due to the general-purpose design of many GROOPS programs, the same programs and force models used, for example, in the processing of LEO satellites can also be used for GNSS satellites. Therefore, any modeling advances in a specific application possibly benefit many other applications.

The main GNSS processing program allows the definition of multiple satellite constellations and station networks with individual parametrizations and models. The resulting system of normal equations is solved by an iterative least squares adjustment. Between each iteration, the weights of the observations are adjusted using variance component estimation, which automatically downweights outliers.

It is possible to fine-tune the processing flow depending on the scale of the task. For example, a small network of 60 stations observing the GPS constellation can be solved directly on a desktop computer. Large-scale processing involving multiple constellations and networks with hundreds of stations may require a different strategy to be solvable even on a high-performance computing cluster. GROOPS has been used to process more than 800 stations and 80 satellites at once, resulting in an equation system with around 200 million observations and 5 million parameters for a single day. A processing flow to solve a system at this scale using GROOPS is described by Strasser et al. (2019).

GNSS solutions produced with GROOPS have been incorporated into the third reprocessing campaign of the IGS (repro3, Rebischung et al., 2019), which constitutes the GNSS contribution to the next International Terrestrial Reference Frame (ITRF2020, Altamimi et al., 2018). The data set produced for repro3 (Strasser and Mayer-Gürr, 2021) covers the years 1994–2020 and is comprised of satellite orbits, station positions, clock errors, signal biases, Earth rotation parameters, tropospheric parameters, satellite attitude, and normal equation systems. Evaluations within the reprocessing campaign show that GROOPS-derived station coordinates and satellite orbits are state of the art (Villiger and Dach, 2020; Rebischung, 2021).

In Fig. 3 we show the difference of station coordinates and satellite orbits processed using GROOPS with respect to the IGS combination. As can be seen, GROOPS-derived GNSS products fit well to the IGS combination, with differences for both stations and satellite orbits on the millimeter to low centimeter level after ambiguity resolution, which is on par with solutions from other IGS analysis centers. More extensive comparisons with products of IGS analysis centers can be found in Strasser et al. (2019).

2.4. Determination of kinematic LEO satellite orbits

Next to the processing of large-scale global station networks, GROOPS also supports precise point positioning (PPP, Zumberge et al., 1997; Martín Furones et al., 2017) of single receivers. PPP can be applied to determine the position of a receiver on Earth's surface or to determine the orbit of an artificial satellite in space (Zehentner and Mayer-Gürr, 2016).

For LEO satellites we can distinguish two types of satellite orbit products. The first type are so-called dynamic orbits, which are based on a force model and then fitted to geometric observations of the satellite, for example, acquired by an onboard GNSS receiver or a satellite laser ranging station. For an optimal fit between the dynamic and actual satellite orbit, the force model must properly describe all forces acting on the satellite. A non-exhaustive list of these forces includes the gravitational attraction of the Earth and other bodies in the solar system, temporal variations in the mass distribution on Earth's surface caused by tidal effects, and non-conservative forces such as atmospheric drag or solar radiation pressure. Combining this model information with observations leads to a, depending on the model quality, smooth and precise representation of the satellite's orbit.

The second type of orbit products are kinematic positions purely derived from geometric measurements. For certain applications, such as gravity field recovery, it is necessary to use these kinematic orbits because dynamic orbits would leak model information, which leads to a bias in derived gravity field products (Gerlach et al., 2003; Jäggi et al., 2008). In GROOPS we use the raw observation approach, that is, only use undifferenced and uncombined GNSS code and phase measurements to determine the kinematic orbit positions. This approach follows the principle of PPP. Known systematic influences are modeled and reduced from the observations, whereas systematic influences that are not known with sufficient accuracy are estimated together with the sought-after satellite positions. The corrected observations are then connected to the unknown parameters, for example ionospheric influence and phase ambiguities, in a least squares adjustment.

The kinematic LEO orbit determination as implemented in GROOPS is designed to handle additional/new satellite missions without major adaptions within the source code. Next to the high-quality measurements of a GNSS receiver aboard the satellite, precise knowledge of the orientation in space, typically collected by star trackers, and information about the GNSS antenna parameters is required for a reasonable kinematic position estimate. So far, kinematic orbits of 14 satellite missions have been computed. These data sets are available at https://ifg.tugraz.at/downloads/satellite-orbit-products/ (last accessed 2020-12-17).

Fig. 4 shows a comparison between kinematic orbit products of the Astronomical Institute at the University of Bern (AIUB) and ambiguity-fixed kinematic orbits computed with GROOPS (ITSG). We derived the monthly 3D root mean square (RMS) presented in the figure by first computing the differences of each product with respect to the L1B reduced-dynamic orbit provided by JPL (JPL, 2001). We then also estimated and removed a once-per-revolution oscillation to account for potential force model errors in the reduced dynamic orbits (Kang et al., 2003) before computing the RMS for each month. As a consequence, the values given in Fig. 4 should be taken as a relative comparison rather than an absolute quantification of the noise level in the kinematic orbits.

GROOPS-derived LEO orbit products have been primarily used as input data for gravity field recovery (da Encarnação et al., 2020; Kvas et al., 2019b) and atmospheric research (Vielberg et al., 2018).

2.5. Data preprocessing and analysis

GROOPS has the capability to analyze and visualize both input data and computed results. This includes Fourier and wavelet transforms of time series data, filtering, computation of sample distributions through histograms, and statistical analysis of spatial and time series data. GROOPS supports the derivation of sample statistics for multivariate time series data like the mean, RMS, standard deviation, minimum/maximum, and median. For comparing two time series, GROOPS can compute the difference RMS, correlation, and the Nash–Sutcliffe coefficient (Nash and Sutcliffe, 1970). Spatial data sets can be analyzed in a similar fashion, however the feature set is smaller than for time series data, specifically for cross-statistics. A notable feature in the handling of spatial data is that if an area element is associated with each point, GROOPS per default computes the area-weighted RMS and area-weighted mean.

One application of such an analysis are post-fit residuals (Goswami et al., 2018; Behzadpour et al., 2019). The example in Fig. 5 shows range-rate residuals of the GRACE-FO laser ranging interferometer (LRI), which we numerically differentiated. For more clarity we excluded all residuals with a magnitude below 0.5 nm s^{-2}. Range-rate observations are originally given as a time series, however, GROOPS offers the possibility to represent the data in different domains. This allows the user to easily identify correlations or artifacts caused by different phenomena. In Fig. 5 the residuals are co-located with the satellite position along the ground track at the time the corresponding measurement was taken. In this domain, we can clearly identify geophysical features such as the magnetic equator or the Argentine gyre.

Next to the analysis of observations or residuals, GROOPS also offers the possibility to visualize and analyze geophysical signals from computed gravity field solutions. One application of such an analysis

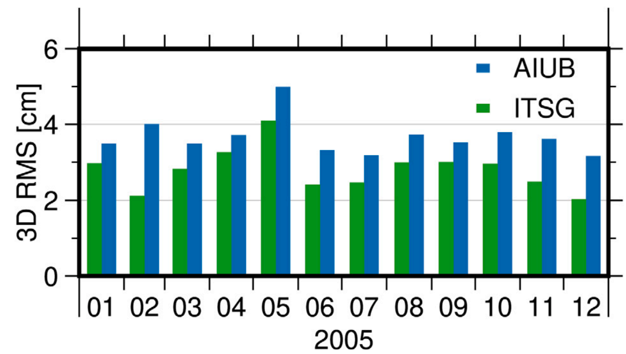

Fig. 4. Monthly 3D RMS of differences between kinematic and dynamic orbit positions for GRACE-A (once-per-revolution oscillation reduced).

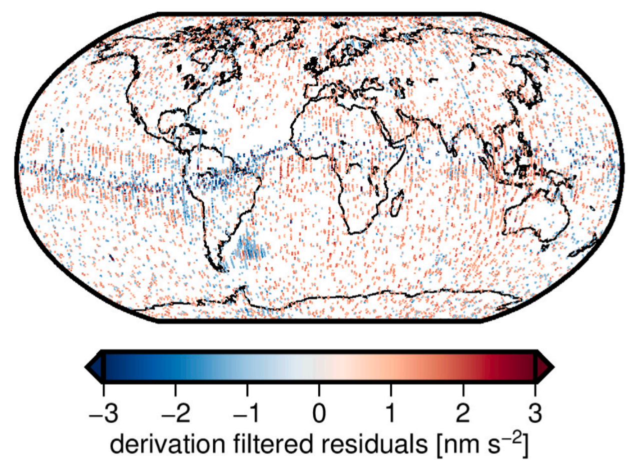

Fig. 5. Derivation-filtered (finite difference approximation of the first derivative) range-rate residuals of the GRACE Follow-On laser ranging interferometer, co-located with the satellite ground track.

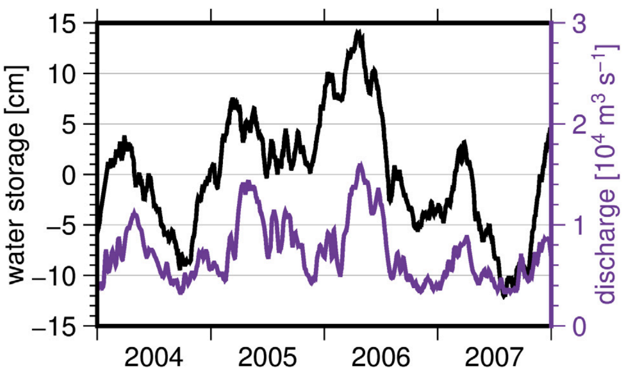

Fig. 6. Time series of Danube basin averages from daily GRACE solutions and discharge data recorded at the river mouth.

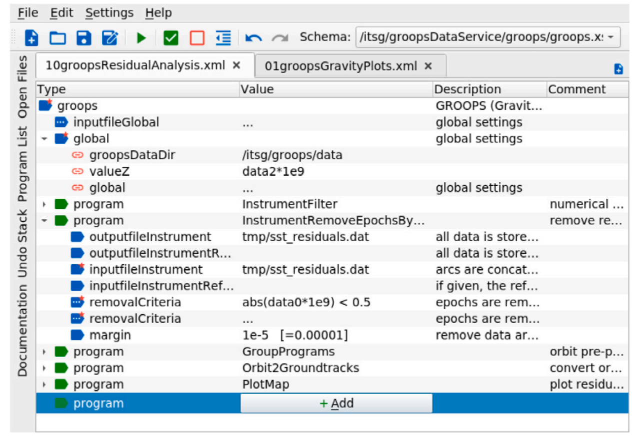

Fig. 7. Screenshot of the GROOPS graphical user interface.

are temporal water storage variations in river basins. In Fig. 6 we show daily basin averages of the Danube derived from GRACE satellite data and compare them with in-situ discharge data which is kindly provided by the Global Runoff Data Centre (GRDC, Global Runoff Data Centre, 2007). GROOPS can not only be used to study individual river basins but also supports the analysis of global data sets. Different applications of global statistics computed and visualized with GROOPS can be found in Eicker et al. (2020).

Data visualization is realized through the Generic Mapping Tools (GMT, Wessel et al., 2019). GMT is not included in the source code, rather GROOPS generates shell or batch scripts which can be passed to the GMT executable. The information content in the different figure types is organized into layers that can be easily created and rearranged in the GUI. Next to data layers, which include line and bar graphs, scatter plots, error bars, and pseudocolor grids, additional annotations such as coast lines or text can be added as layers in the different plotting programs. This enables a flexible composition of publication-quality figures.

3. Software description

3.1. Dependencies

While GROOPS is intended to be a standalone software package, some functionality depends on external libraries. Dependencies are the Expat XML parser (https://libexpat.github.io, last accessed 25-08-2020), routines of the International Earth Rotation and Reference Systems Service Software Collection (Petit and Luzum, 2010), the Jacchia-Bowman 2008 Empirical Thermospheric Density Model (Bowman et al., 2008), the horizontal wind model (HWM14, Drob et al., 2015), the empirical atmospheric model NRLMSIS 2.0 (Emmert et al., 2021), the International Geomagnetic Reference Field (IGRF, Thébault et al., 2015) and an implementation of the Linear Algebra Package (LAPACK, Anderson et al., 1999).

Additional libraries extend the feature set of GROOPS and can be optionally enabled at compile time. At the moment, these include NetCDF (https://unidata.ucar.edu/software/netcdf, last accessed 25-08-2020) for reading and writing NetCDF files, zlib (https://zlib.net, last accessed 25-08-2020) for reading and writing compressed files, and the Essential Routines for Fundamental Astronomy (https://github.com/liberfa/erfa, last accessed 25-08-2020) for high-precision Earth rotation. Another optional dependency is an implementation of the Message Passing Interface (MPI) standard. Resource intensive tasks and algorithms are designed and implemented to be optionally run in parallel on distributed systems. If an MPI implementation is available, GROOPS can be compiled as an MPI executable and either run on a local desktop machine with multiple processes or on a large high-performance computing cluster.

The graphical user interface included in GROOPS is built using the Qt toolkit (https://qt.io, last accessed 25-08-2020), which enables it to be run on various operating systems.

3.2. Software usage

User interaction with GROOPS is based on XML configuration files typically generated in the GUI. Configuration files are written to disk and can then be passed onto the GROOPS executable either directly in the GUI or through the command line. This split between user interaction and execution allows GROOPS to be run on systems without support for GUIs such as high-performance computing clusters.

A configuration file represents a sequence of smaller tasks, dubbed "programs", which comprise a workflow. Programs vary in complexity, but mostly represent atomic operations on data, for example removing trends or resampling a time series. These elementary building blocks allow the user to create flexible processing chains where individual processing steps can be added, removed, or adapted. This modular approach allows programs to be used in different contexts and applications. For example, data preprocessing and outlier removal is usually very similar for different satellite missions and also shares common steps with GNSS processing.

Fig. 7 shows an example of a configuration file as depicted in the GUI. This example covers a typical workflow for data analysis. In a first step, post-fit residuals of inter-satellite ranging measurements are numerically differentiated by applying a corresponding digital filter to the time series in the program *InstrumentFilter*. Then, values below 0.5 nm s^{-2} are removed through *InstrumentRemoveEpochsByCriteria* to only show large outliers in the data. To see if any geophysical signals are present in the remaining residuals, we want to analyze the time series in space rather than in time domain. To this end, we compute the satellite ground tracks on Earth's surface from the satellite orbit and co-locate the corresponding residual epochs in *Orbit2Groundtracks*. Finally, the now georeferenced residuals are visualized on a global map through *PlotMap*. The result of this workflow is shown in Fig. 5.

Interaction between programs is file-based, that is, a program reads one or more input files, performs its designed task and generates one or more output files which can then be processed by a subsequent program. To make batch processing of large data sets easier, configuration files also support control flow statements such as loops and conditions. Loops can be used to iterate over points in time or file lists and can involve multiple programs. Each loop type sets a number of variables which are updated in each iteration. These variables are resolved at run time and can be used to process, for example, file names with varying time stamps. With conditional execution, missing input data files or different processing requirements can be accounted for.

3.3. Extensibility

The modular structure of the GROOPS configuration files is also reflected in the source code, in that it is object-oriented and designed to be easily extendable. The source code can be categorized into two parts. Low-level functionality is provided by classes in the core library, which includes, for example, matrix multiplication, file input/output, and polynomial interpolation. The second part are the programs, which combine different functionalities from the core library. They can be thought of as plugins or add-ons and are the interface between the software and user. The source code repository includes a program template which can be used as a starting point for tasks that cannot be realized with the included programs.

4. Summary

Data sets that describe Earth's geometric shape, orientation in space, and gravity field provide the basis for a broad range of applications in Earth and environmental sciences. In this article we presented GROOPS, a software toolkit which is capable of computing these quantities with state-of-the-art methods. The software features include gravity field recovery, GNSS constellation and ground station processing, the determination of LEO satellite orbits, and the analysis and visualization of time series and spatial data sets.

The source code, documentation, guided examples, and installation instructions are publicly available on GitHub (https://github.com/groops-devs/groops). An included graphical user interface allows an easy setup of complex workflows for core geodetic tasks and the analysis of geophysical data sets.

GROOPS offers the possibility to compute geodetic data sets from scratch and thus enables researchers to set up processing chains from raw measurement data to the scientific analysis, with full control over each step. Additionally, the publicly available software source code in conjunction with traditionally published documentation provides a comprehensive description of data sets computed with GROOPS. This makes the data generation process transparent and allows users to build upon or adapt existing processing chains to their specific needs. These two aspects make GROOPS a valuable tool for a range of potential users in different Earth and environmental science disciplines.

As a future extension to GROOPS, we plan to implement the handling of satellite laser ranging (SLR) observation data. The modular software design ensures that much functionality, such as outlier detection or dynamic orbit integration, can be shared between all observation techniques. Thus, the majority of the required work will be to implement correction models for the SLR measurements, partial derivatives with respect to SLR specific calibration parameters for both satellites and stations, and the proper handling of station and satellite meta data. Having a third space geodetic technique available will allow users to perform cross-validations or observation combination without the need for external tools.

CRediT authorship contribution statement

Torsten Mayer-Gürr: Lead developer of GROOPS and initial design of the software, developed and implemented methods, wrote documentation and usage guide. **Saniya Behzadpour:** Developed and implemented methods, contributed to the software in the form of methods, source code and/or documentation, wrote documentation and usage guide. **Annette Eicker:** Developed and implemented methods, contributed to the software in the form of methods, wrote documentation and usage guide. **Matthias Ellmer:** Developed and implemented methods, contributed to the software in the form of methods, wrote documentation and usage guide. **Beate Koch:** Developed and implemented methods, contributed to the software in the form of methods, wrote documentation and usage guide. **Sandro Krauss:** Developed and implemented methods, contributed to the software in the form of methods, wrote documentation and usage guide. **Christian Pock:** Developed and implemented methods, contributed to the software in the form of methods, wrote documentation and usage guide. **Daniel Rieser:** Developed and implemented methods, contributed to the software in the form of methods, wrote documentation and usage guide. **Sebastian Strasser:** Developed and implemented methods, contributed to the software in the form of methods, wrote documentation and usage guide, Wrote the manuscript. **Barbara Süsser-Rechberger:** Developed and implemented methods, contributed to the software in the form of methods, wrote documentation and usage guide. **Norbert Zehentner:** Developed and implemented methods, contributed to the software in the form of methods, wrote documentation and usage guide. **Andreas Kvas:** Developed and implemented methods, contributed to the software in the form of methods, wrote documentation and usage guide, wrote the manuscript.

Declaration of competing interest

The authors declare that they have no known competing financial interests or personal relationships that could have appeared to influence the work reported in this paper.

Acknowledgments

Parts of GROOPS originate from developments in the Astronomical, Physical and Mathematical Geodesy Group at the University of Bonn, Germany. Since 2010 it is developed and maintained at Graz University of Technology, Austria.

We thank the three anonymous reviewers for providing insightful comments which helped us improve the manuscript. Supported by TU Graz Open Access Publishing Fund.

References

Altamimi, Z., Rebischung, P., Collilieux, X., Metivier, L., Chanard, K., 2018. Roadmap toward ITRF2020. Abstract G42A-08, presented at 2018 Fall Meeting, AGU, Washington, D. C., 10-14 Dec.

Anderson, E., Bai, Z., Bischof, C., Blackford, S., Demmel, J., Dongarra, J., Du Croz, J., Greenbaum, A., Hammarling, S., McKenney, A., Sorensen, D., 1999. LAPACK Users' Guide, third ed. Society for Industrial and Applied Mathematics, Philadelphia, PA.

Asif, A., Moura, J.M.F., 2005. Block matrices with L-block-banded inverse: inversion algorithms. IEEE Trans. Signal Process. 53 (2), 630–642. http://dx.doi.org/10.1109/TSP.2004.840709.

Baur, O., 2009. Tailored least-squares solvers implementation for high-performance gravity field research. Comput. Geosci. 35 (3), 548–556. http://dx.doi.org/10.1016/j.cageo.2008.09.004, URL: https://www.sciencedirect.com/science/article/pii/S0098300408002628.

Behzadpour, S., Mayer-Gürr, T., Flury, J., Klinger, B., Goswami, S., 2019. Multiresolution wavelet analysis applied to GRACE range-rate residuals. Geosci. Instrum. Methods Data Syst. 8 (2), 197–207. http://dx.doi.org/10.5194/gi-8-197-2019.

Bertiger, W., Bar-Sever, Y., Dorsey, A., Haines, B., Harvey, N., Hemberger, D., Heflin, M., Lu, W., Miller, M., Moore, A.W., Murphy, D., Ries, P., Romans, L., Sibois, A., Sibthorpe, A., Szilagyi, B., Vallisneri, M., Willis, P., 2020. GipsyX/RTGx, a new tool set for space geodetic operations and research. Adv. Space Res. 66 (3), 469–489. http://dx.doi.org/10.1016/j.asr.2020.04.015.

Bingham, R.J., Haines, K., Lea, D.J., 2014. How well can we measure the ocean's mean dynamic topography from space? J. Geophys. Res. Oceans 119 (6), 3336–3356. http://dx.doi.org/10.1002/2013JC009354.

Blackford, L.S., Choi, J., Cleary, A., D'Azeuedo, E., Demmel, J., Dhillon, I., Hammarling, S., Henry, G., Petitet, A., Stanley, K., Walker, D., Whaley, R.C., Dongarra, J.J., 1997. ScaLAPACK User's Guide. Society for Industrial and Applied Mathematics, USA.

Blewitt, G., Altamimi, Z., Davis, J., Gross, R., Kuo, C.Y., Lemoine, F.G., Moore, A.W., Neilan, R.E., Plag, H.P., Rothacher, M., Shum, C.K., Sideris, M.G., Schöne, T., Tregoning, P., Zerbini, S., 2010. Geodetic observations and global reference frame contributions to understanding sea-level rise and variability. In: Understanding Sea-Level Rise and Variability. John Wiley & Sons, Ltd, pp. 256–284. http://dx.doi.org/10.1002/9781444323276.ch9.

Böhm, J., Böhm, S., Boisits, J., Girdiuk, A., Gruber, J., Hellerschmied, A., Krásná, H., Landskron, D., Madzak, M., Mayer, D., McCallum, J., McCallum, L., Schartner, M., Teke, K., 2018. Vienna VLBI and satellite software (VieVS) for geodesy and astrometry. Publ. Astron. Soc. Pac. 130 (986), 44503. http://dx.doi.org/10.1088/1538-3873/aaa22b.

Bonin, J.A., Save, H., 2020. Evaluation of sub-monthly oceanographic signal in GRACE "daily" swath series using altimetry. Ocean Sci. 16 (2), 423–434. http://dx.doi.org/10.5194/os-16-423-2020.

Bowman, B., Tobiska, W.K., Marcos, F., Huang, C., Lin, C., Burke, W., 2008. A new empirical thermospheric density model JB2008 using new solar and geomagnetic indices. In: AIAA/AAS Astrodynamics Specialist Conference and Exhibit. http://dx.doi.org/10.2514/6.2008-6438.

Boxhammer, C., Schuh, W.D., 2006. GOCE gravity field modeling: Computational aspects — Free kite numbering scheme. In: Flury, J., Rummel, R., Reigber, C., Rothacher, M., Boedecker, G., Schreiber, U. (Eds.), Observation of the Earth System from Space. Springer Berlin Heidelberg, Berlin, Heidelberg, pp. 209–224. http://dx.doi.org/10.1007/3-540-29522-4_15.

Chambers, D.P., 2006. Observing seasonal steric sea level variations with GRACE and satellite altimetry. J. Geophys. Res. Oceans 111, http://dx.doi.org/10.1029/2005JC002914.

Chen, J.L., Wilson, C.R., Tapley, B.D., 2010. The 2009 exceptional amazon flood and interannual terrestrial water storage change observed by GRACE. Water Resour. Res. 46 (12), http://dx.doi.org/10.1029/2010WR009383.

Choi, J., Dongarra, J.J., Ostrouchov, L.S., Petitet, A.P., Walker, D.W., Whaley, R.C., 1996. Design and implementation of the ScaLAPACK LU, QR, and Cholesky factorization routines. Sci. Program. 5 (3), 173–184. http://dx.doi.org/10.1155/1996/483083.

Cooper, H.M., Zhang, C., Davis, S.E., Troxler, T.G., 2019. Object-based correction of LiDAR DEMs using RTK-GPS data and machine learning modeling in the coastal everglades. Environ. Model. Softw. 112, 179–191. http://dx.doi.org/10.1016/j.envsoft.2018.11.003.

Dach, R., Lutz, S., Walser, P., Fridez, P., 2015. Bernese GNSS Software Version 5.2. Technical Report, Astronomical Institute, University of Bern, Bern, http://dx.doi.org/10.7892/boris.72297.

Drob, D.P., Emmert, J.T., Meriwether, J.W., Makela, J.J., Doornbos, E., Conde, M., Hernandez, G., Noto, J., Zawdie, K.A., McDonald, S.E., Huba, J.D., Klenzing, J.H., 2015. An update to the Horizontal Wind Model (HWM): The quiet time thermosphere. Earth Space Sci. 2 (7), 301–319. http://dx.doi.org/10.1002/2014EA000089.

Ebbing, J., Haas, P., Ferraccioli, F., Pappa, F., Szwillus, W., Bouman, J., 2018. Earth tectonics as seen by GOCE - Enhanced satellite gravity gradient imaging. Sci. Rep. 8 (1), 16356. http://dx.doi.org/10.1038/s41598-018-34733-9.

Eicker, A., Jensen, L., Wöhnke, V., Dobslaw, H., Kvas, A., Mayer-Gürr, T., Dill, R., 2020. Daily GRACE satellite data evaluate short-term hydro-meteorological fluxes from global atmospheric reanalyses. Sci. Rep. 10 (1), 4504. http://dx.doi.org/10.1038/s41598-020-61166-0.

Eicker, A., Schall, J., Kusche, J., 2013. Regional gravity modelling from spaceborne data: case studies with GOCE. Geophys. J. Int. 196 (3), 1431–1440. http://dx.doi.org/10.1093/gji/ggt485.

Ellmer, M., 2018. Contributions to GRACE Gravity Field Recovery: Improvements in Dynamic Orbit Integration Stochastic Modelling of the Antenna Offset Correction, and Co-Estimation of Satellite Orientations (Ph.D. thesis). In: Monographic Series TU Graz, (1), Graz University of Technology, http://dx.doi.org/10.3217/978-3-85125-646-8.

Ellmer, M., Mayer-Gürr, T., 2017. High precision dynamic orbit integration for spaceborne gravimetry in view of GRACE follow-on. Adv. Space Res. 60 (1), 1–13. http://dx.doi.org/10.1016/j.asr.2017.04.015.

Emmert, J.T., Drob, D.P., Picone, J.M., Siskind, D.E., Jones, Jr., M., Mlynczak, M.G., Bernath, P.F., Chu, X., Doornbos, E., Funke, B., Goncharenko, L.P., Hervig, M.E., Schwartz, M.J., Sheese, P.E., Vargas, F., Williams, B.P., Yuan, T., 2021. NRLMSIS 2.0: A whole-atmosphere empirical model of temperature and neutral species densities. Earth Space Sci. 8 (3), http://dx.doi.org/10.1029/2020EA001321, e2020EA001321.

da Encarnação, J., Visser, P., Arnold, D., Bezdek, A., Doornbos, E., Ellmer, M., Guo, J., van den IJssel, J., Iorfida, E., Jäggi, A., Klokocník, J., Krauss, S., Mao, X., Mayer-Gürr, T., Meyer, U., Sebera, J., Shum, C.K., Zhang, C., Zhang, Y., Dahle, C., 2020. Description of the multi-approach gravity field models from Swarm GPS data. Earth Syst. Sci. Data 12 (2), 1385–1417. http://dx.doi.org/10.5194/essd-12-1385-2020.

Gerlach, C., Földvary, L., Švehla, D., Gruber, T., Wermuth, M., Sneeuw, N., Frommknecht, B., Oberndorfer, H., Peters, T., Rothacher, M., Rummel, R., Steigenberger, P., 2003. A CHAMP-only gravity field model from kinematic orbits using the energy integral. Geophys. Res. Lett. 30 (20), http://dx.doi.org/10.1029/2003GL018025, URL: https://doi.org/10.1029/2003GL018025.

Ghobadi-Far, K., Han, S.C., McCullough, C.M., Wiese, D.N., Yuan, D.-N., Landerer, F.W., Sauber, J., Watkins, M.M., 2020. GRACE follow-on laser ranging interferometer measurements uniquely distinguish short-wavelength gravitational perturbations. Geophys. Res. Lett. 47 (16), http://dx.doi.org/10.1029/2020GL089445, e2020GL089445.

Global Runoff Data Centre, 2007. River Discharge Data. Technical Report, Federal Institute of Hydrology (BfG), Koblenz, Germany.

Goswami, S., Devaraju, B., Weigelt, M., Mayer-Gürr, T., Behzadpour, S., 2018. Analysis of GRACE range-rate residuals with focus on KBR instrument system noise. Adv. Space Res. 62 (2), 304–316. http://dx.doi.org/10.1016/j.asr.2018.04.036.

Goto, K., van de Geijn, R., 2006. High-performance implementation of the level-3 BLAS. ACM Trans. Math. Software 35, http://dx.doi.org/10.1145/1377603.1377607.

Göttl, F., Murböck, M., Schmidt, M., Seitz, F., 2019. Reducing filter effects in GRACE-derived polar motion excitations. Earth Planets Space 71 (1), 117. http://dx.doi.org/10.1186/s40623-019-1101-z.

Gouweleeuw, B.T., Kvas, A., Gruber, C., Gain, A.K., Mayer-Gürr, T., Flechtner, F., Güntner, A., 2018. Daily GRACE gravity field solutions track major flood events in the Ganges–Brahmaputra Delta. Hydrol. Earth Syst. Sci. 22 (5), 2867–2880. http://dx.doi.org/10.5194/hess-22-2867-2018.

Harpham, Q., Tozer, N., Cleverley, P., Wyncoll, D., Cresswell, D., 2016. A Bayesian method for improving probabilistic wave forecasts by weighting ensemble members. Environ. Model. Softw. 84, 482–493. http://dx.doi.org/10.1016/j.envsoft.2016.07.015.

Hirt, C., Kuhn, M., Claessens, S., Pail, R., Seitz, K., Gruber, T., 2014. Study of the Earth's short-scale gravity field using the ERTM2160 gravity model. Comput. Geosci. 73, 71–80. http://dx.doi.org/10.1016/j.cageo.2014.09.001, URL: https://www.sciencedirect.com/science/article/pii/S0098300414002039.

Humphrey, V., Gudmundsson, L., 2019. GRACE-REC: a reconstruction of climate-driven water storage changes over the last century. Earth Syst. Sci. Data 11 (3), 1153–1170. http://dx.doi.org/10.5194/essd-11-1153-2019.

Jäggi, A., Bock, H., Pail, R., Goiginger, H., 2008. Highly-reduced dynamic orbits and their use for global gravity field recovery: A simulation study for GOCE. Stud. Geophys. Geod. 52 (3), 341–359. http://dx.doi.org/10.1007/s11200-008-0025-z, URL: https://doi.org/10.1007/s11200-008-0025-z.

Jäggi, A., Meyer, U., Lasser, M., Jenny, B., Lopez, T., Flechtner, F., Dahle, C., Förste, C., Mayer-Gürr, T., Kvas, A., Lemoine, J.-M., Bourgogne, S., Weigelt, M., Groh, A., 2020. International combination service for time-variable gravity fields (COST-G): Start of operational phase and future perspectives. In: International Association of Geodesy Symposia. Springer Nature, pp. 1–9. http://dx.doi.org/10.1007/1345_2020_109.

Johannessen, J.A., Balmino, G., Provost, C.L., Rummel, R., Sabadini, R., Sünkel, H., Tscherning, C.C., Visser, P., Woodworth, P., Hughes, C., Legrand, P., Sneeuw, N., Perosanz, F., Aguirre-Martinez, M., Rebhan, H., Drinkwater, M., 2003. The European gravity field and steady-state ocean circulation explorer satellite mission its impact on geophysics. Surv. Geophys. 24 (4), 339–386. http://dx.doi.org/10.1023/B:GEOP.0000004264.04667.5e.

Johnston, G., Riddell, A., Hausler, G., 2017. The international GNSS service. In: Teunissen, P.J.G., Montenbruck, O. (Eds.), Springer Handbook of Global Navigation Satellite Systems. Springer International Publishing, Cham, pp. 967–982. http://dx.doi.org/10.1007/978-3-319-42928-1_33.

JPL, 2001. GRACE LEVEL 1B JPL RELEASE 2.0. http://dx.doi.org/10.5067/GRJPL-L1B02, URL: http://podaac.jpl.nasa.gov/dataset/GRACE_L1B_GRAV_JPL_RL02.

Kang, Z., Nagel, P., Pastor, R., 2003. Precise orbit determination for GRACE. Adv. Space Res. 31 (8), 1875–1881. http://dx.doi.org/10.1016/S0273-1177(03)00159-5, URL: https://www.sciencedirect.com/science/article/pii/S0273117703001595.

Koch, K.R., Kusche, J., 2002. Regularization of geopotential determination from satellite data by variance components. J. Geod. 76 (5), 259–268. http://dx.doi.org/10.1007/s00190-002-0245-x.

Kvas, A., 2020. Estimation of High-Frequency Mass Variations from Satellite Data in near Real-Time: Implementation of a Technology Demonstrator for near Real-Time GRACE/GRACE-FO Gravity Field Solutions (Ph.D. thesis). Graz University of Technology, http://dx.doi.org/10.3217/978-3-85125-771-7.

Kvas, A., Behzadpour, S., Ellmer, M., Klinger, B., Strasser, S., Zehentner, N., Mayer-Gürr, T., 2019a. ITSG-Grace2018: Overview and evaluation of a new GRACE-only gravity field time series. J. Geophys. Res. Solid Earth 124 (8), 9332–9344. http://dx.doi.org/10.1029/2019JB017415.

Kvas, A., Brockmann, J.M., Krauss, S., Schubert, T., Gruber, T., Meyer, U., Mayer-Gürr, T., Schuh, W.D., Jäggi, A., Pail, R., 2020. GOCO06s – A satellite-only global gravity field model. Earth Syst. Sci. Data Discuss. 2020, 1–31. http://dx.doi.org/10.5194/essd-2020-192.

Kvas, A., Mayer-Gürr, T., 2019. GRACE gravity field recovery with background model uncertainties. J. Geod. 93 (12), 2543–2552. http://dx.doi.org/10.1007/s00190-019-01314-1.

Kvas, A., Mayer-Gürr, T., Krauss, S., Brockmann, J.M., Schubert, T., Schuh, W.D., Pail, R., Gruber, T., Jäggi, A., Meyer, U., 2019b. The satellite-only gravity field model GOCO06s. http://dx.doi.org/10.5880/ICGEM.2019.002.

Le Cozannet, G., Rohmer, J., Cazenave, A., Idier, D., van de Wal, R., de Winter, R., Pedreros, R., Balouin, Y., Vinchon, C., Oliveros, C., 2015. Evaluating uncertainties of future marine flooding occurrence as sea-level rises. Environ. Model. Softw. 73, 44–56. http://dx.doi.org/10.1016/j.envsoft.2015.07.021.

Martín Furones, A., Anquela Julián, A.B., Dimas-Pages, A., Cos-Gayón, F., 2017. Computational time reduction for sequential batch solutions in GNSS precise point positioning technique. Comput. Geosci. 105, 34–42. http://dx.doi.org/10.1016/j.cageo.2017.03.023, URL: https://www.sciencedirect.com/science/article/pii/S0098300416306318.

Mayer-Gürr, T., 2006. Gravitationsfeldbestimmung aus der Analyse kurzer Bahnbögen am Beispiel der Satellitenmissionen CHAMP und GRACE (Ph.D. thesis). University of Bonn, Germany, URL: http://hdl.handle.net/20.500.11811/1391.

Meyer, U., Jean, Y., Kvas, A., Dahle, C., Lemoine, J., Jäggi, A., 2019. Combination of GRACE monthly gravity fields on the normal equation level. J. Geod. http://dx.doi.org/10.1007/s00190-019-01274-6.

Montenbruck, O., Gill, E., 2000. Satellite Orbits. Springer-Verlag Berlin Heidelberg New York.

Nash, J.E., Sutcliffe, J.V., 1970. River flow forecasting through conceptual models part I — A discussion of principles. J. Hydrol. 10 (3), 282–290. http://dx.doi.org/10.1016/0022-1694(70)90255-6.

Nerem, R.S., Eanes, R.J., Ries, J.C., Mitchum, G.T., 2000. The use of a precise reference frame in sea level change studies. In: Rummel, R., Drewes, H., Bosch, W., Hornik, H. (Eds.), Towards an Integrated Global Geodetic Observing System. IGGOS, Springer Berlin Heidelberg, Berlin, Heidelberg, pp. 8–12.

Petit, G., Luzum, B. (Eds.), 2010. IERS Conventions (2010). Verlag des Bundesamts für Kartographie und Geodäsie, Frankfurt am Main.

Pock, C., Mayer-Guerr, T., Kuehtreiber, N., 2014. Consistent combination of satellite and terrestrial gravity field observations in regional geoid modeling: A case study for Austria. In: Marti, U. (Ed.), Gravity, Geoid and Height Systems. Springer International Publishing, Cham, pp. 151–156.

Rebischung, P., 2021. Terrestrial frame solutions from the IGS third reprocessing. http://dx.doi.org/10.5194/egusphere-egu21-2144, Abstract EGU21-2144, presented at EGU General Assembly 2021, online, 19–30 Apr 2021.

Rebischung, P., Villiger, A., Herring, T., Moore, M., 2019. Preliminary results from the third IGS reprocessing campaign. Abstract G11A-03, presented at 2019 Fall Meeting, AGU, San Francisco, CA, 9-13 Dec..

Schönemann, E., 2014. Analysis of GNSS raw observations in PPP solutions. In: Schriftenreihe der Fachrichtung Geodäsie, Vol. 42, Darmstadt. URL: https://tuprints.ulb.tu-darmstadt.de/3843/.

Schönemann, E., Becker, M., Springer, T., 2011. A new approach for GNSS analysis in a multi-GNSS and multi-signal environment. J. Geod. Sci. 1 (3), 204–214. http://dx.doi.org/10.2478/v10156-010-0023-2.

Schuh, W., 1996. Tailored Numerical Solution Strategies for the Global Determination of the Earth'S Gravity Field: Study of the Complementary Use of the Gradiometry and Global Positioning System (GPS) for the Determination of the Earth'S Gravity Field. Technical Report, In: Mitteilungen der Geodätischen Institute der Technischen Universität Graz / Mitteilungen der Geodätischen Institute der Technischen Universität Graz, Techn. Univ. Graz, Inst. für Theoret. Geodäsie, URL: https://books.google.com/books?id=98FmxgEACAAJ.

Strasser, S., Mayer-Gürr, T., 2021. IGS repro3 products by Graz University of Technology (TUG).

Strasser, S., Mayer-Gürr, T., Zehentner, N., 2019. Processing of GNSS constellations and ground station networks using the raw observation approach. J. Geod. 93 (7), 1045–1057. http://dx.doi.org/10.1007/s00190-018-1223-2.

Tapley, B.D., Watkins, M.M., Flechtner, F., Reigber, C., Bettadpur, S., Rodell, M., Sasgen, I., Famiglietti, J.S., Landerer, F.W., Chambers, D.P., Reager, J.T., Gardner, A.S., Save, H., Ivins, E.R., Swenson, S.C., Boening, C., Dahle, C., Wiese, D.N., Dobslaw, H., Tamisiea, M.E., Velicogna, I., 2019. Contributions of GRACE to understanding climate change. Nature Clim. Change 9 (5), 358–369. http://dx.doi.org/10.1038/s41558-019-0456-2.

Tewarson, R.P., Cheng, K.Y., 1973. A desirable form for sparse matrices when computing their inverse in factored forms. Computing 11 (1), 31–38. http://dx.doi.org/10.1007/BF02239469, URL: https://doi.org/10.1007/BF02239469.

Thébault, E., Finlay, C.C., Beggan, C.D., Alken, P., Aubert, J., Barrois, O., Bertrand, F., Bondar, T., Boness, A., Brocco, L., Canet, E., Chambodut, A., Chulliat, A., Coïsson, P., Civet, F., Du, A., Fournier, A., Fratter, I., Gillet, N., Hamilton, B., Hamoudi, M., Hulot, G., Jager, T., Korte, M., Kuang, W., Lalanne, X., Langlais, B., Léger, J.M., Lesur, V., Lowes, F.J., Macmillan, S., Mandea, M., Manoj, C., Maus, S., Olsen, N., Petrov, V., Ridley, V., Rother, M., Sabaka, T.J., Saturnino, D., Schachtschneider, R., Sirol, O., Tangborn, A., Thomson, A., Tøffner-Clausen, L., Vigneron, P., Wardinski, I., Zvereva, T., 2015. International geomagnetic reference field: the 12th generation. Earth Planets Space 67 (1), 79. http://dx.doi.org/10.1186/s40623-015-0228-9.

Velicogna, I., 2009. Increasing rates of ice mass loss from the Greenland and Antarctic ice sheets revealed by GRACE. Geophys. Res. Lett. 36 (19), http://dx.doi.org/10.1029/2009GL040222.

Vielberg, K., Forootan, E., Lück, C., Löcher, A., Kusche, J., Börger, K., 2018. Comparison of accelerometer data calibration methods used in thermospheric neutral density estimation. Ann. Geophys. 36 (3), 761–779. http://dx.doi.org/10.5194/angeo-36-761-2018.

Villiger, A., Dach, R., 2020. International GNSS Service: Technical Report 2019. Technical Report, IGS Central Bureau and University of Bern Open Publishing, http://dx.doi.org/10.7892/boris.144003.

Wessel, P., Luis, J.F., Uieda, L., Scharroo, R., Wobbe, F., Smith, W.H.F., Tian, D., 2019. The generic mapping tools version 6. Geochem. Geophys. Geosyst. 20 (11), 5556–5564. http://dx.doi.org/10.1029/2019GC008515.

Wirnsberger, H., Krauss, S., Mayer-Gürr, T., 2019. First independent graz lunar gravity model derived from GRAIL. Icarus 317, 324–336. http://dx.doi.org/10.1016/j.icarus.2018.08.011.

Zehentner, N., Mayer-Gürr, T., 2016. Precise orbit determination based on raw GPS measurements. J. Geod. 90 (3), 275–286. http://dx.doi.org/10.1007/s00190-015-0872-7.

Zumberge, J.F., Heflin, M.B., Jefferson, D.C., Watkins, M.M., Webb, F.H., 1997. Precise point positioning for the efficient and robust analysis of GPS data from large networks. J. Geophys. Res. Solid Earth 102 (B3), 5005–5017. http://dx.doi.org/10.1029/96jb03860.